Fibers and Polymers
https://doi.org/10.1007/s12221-026-01550-1

Online ISSN 1875-0052
Print ISSN 1229-9197

REGULAR ARTICLE

Production and Influence of SiO_2 and Fiber Sequencing on the Mechanical and Thermal Properties of Kenaf/Sisal/Glass Laminates

C. Gnanavel[1] · Sathukumati Leela Lakshmi[2] · Nirmith Kumar Mishra[3] · Ayinala Naga Sai[4] · S. Karvendhan[5] · S. Prabagaran[6] · S. Jothi Arunachalam[7] · Ramya Maranan[8] · Anand Rajendran[9] · S. Sathiyamurthy[10]

Received: 27 February 2026 / Revised: 2 August 2026 / Accepted: 11 August 2026

Abstract
The epoxy-fiber composite laminates are found to have a high strength-to-weight ratio, enhanced fatigue strength, and better stiffness performance. However, weak interfacial bonding, improved moisture absorption, and brittle nature due to higher epoxy content limit the overall functional properties of the composites. The objectives of the present research are to produce and enhance the functional properties of the Kenaf (KF)–sisal (SF)–glass fiber (GF)-reinforced epoxy composite laminates fabricated with 3 wt% nano-silicon dioxide (SiO_2) via hot compression molding production method. During the fabrication, the 0/0/0 degree, 45/0/0 degree, 0/45/0 degree, and 0/0/45 degree laminates were formed without and with 3 wt% SiO_2. The effect of the fiber laminate and SiO_2 on X-ray diffraction analysis, mechanical properties, moisture absorption, and thermogravimetric analysis of the composites was studied. The epoxy hybrid composite laminate of 0/45/0 with 3 wt% SiO_2 nanoparticles showed a higher tensile strength of 92.2 MPa, improved flexural strength of 145 MPa, better impact strength of 31 kJ/m^2, and reduced water absorption of 2.4%. Furthermore, thermogravimetric analysis (TGA) demonstrated that the introduction of SiO_2 enhanced the onset decomposition temperature, and the moisture uptake tests recorded a significant decrease in water uptake, favoring dimensional stability.

Keywords Epoxy-fiber composite laminates · Hot compression · Moisture absorption · Production · Tensile strength · Thermogravimetric analysis

1 Introduction

In the past few years, fiber-reinforced polymer (FRP) composites have received much attention because of their high mechanical performance, low weight density, and resistance to corrosion, which has made them ideal for structural, automotive, and aerospace structures [1]. Among others, hybrid composites, which are natural and synthetic fiber, have come out as an alternative promising substitute to conventional composites, which allows optimization of mechanical strength, reduced weight, and better environmentally sustainable [2]. Natural fibers such as kenaf and sisal are renewable, economical and have good specific strength, but the absorption characteristics of moisture, as well as thermal stability of these fibers, tend to limit their high-performance use [3, 4]. To eliminate these demerits, polymerization with synthetic fibers such as glass fiber and the use of nanofilled are viable techniques of improving the properties. SiO_2 nanoparticles have been extensively utilized as nanoscale reinforcements because they are very stiff, thermally stable and enhance the fiber–matrix interfacial bonding [5]. Polymer chain mobility can be limited by incorporation of well-dispersed SiO_2 that enhances mechanical strength, stiffness, and thermal degradation resistance [6]. Also, the arrangement of fibers in the stack of hybrid laminates is significant in determining the load transfer efficiency, failure behavior, and anisotropic behavior when subjected to external forces. The optimization of this fiber orientation sequence may have a great impact on the stiffness of the composites, flexural strength, and the overall durability [7].

Introduction of SiO_2 nanoparticles has proven to play a great role in interfacial bonding, which results in better mechanical properties, including tensile strength, flexural strength and hardness, and thermal stability of hybrid composites [8]. An example is a composite specimen (S4, 5%) of

Extended author information available on the last page of the article

Published online: 20 August 2026

jute/kenaf/glass fibers that are infused with SiO_2, nanographene, and multi-walled carbon nanotubes (MWCNTs) that exhibited greater tensile strength [9]. In another research using SiO_2 as an intermediate layer in jute/kenaf/glass fiber composite hybrid, the functional properties were improved. It was revealed that the silane coating of the granite dust particles, which are quartz-rich SiO_2, enhances interfacial bonding and dispersion of the aluminized glass–kenaf fiber-reinforced polyester composites, which have an effect on the load-bearing properties, water absorption properties, and flame properties [10]. In the same way, nano-biosilica prepared using sorghum husk when impregnated with silane-treated kenaf fiber improved such mechanical properties as tensile, flexural, and compression strength, Izod impact toughness, hardness, fatigue life, and creep resistance. This was done by mixing the silane solution using 3-aminopropyltrimethoxysilane (APTMs) to alter the surface of kenaf fiber and nano-biosilica to make them more compatible in composite applications [11]. Arrangements of fiber sequencing and stacking are important in the optimization of the mechanical and thermal behavior of hybrid laminates.

A study on kenaf/jute fiber-reinforced polyester hybrid biocomposites that employed the various order arrangements of stacking showed varied mechanical and thermal properties [12]. Through the incorporation of glass fiber with kenaf in particular stacking arrangement can enhance mechanical properties, including tensile and flexural strength significantly [13]. Research on woven kenaf/polyester-reinforced polylactic acid hybrid laminated composites experimented with the influence of fiber content and stacking order on thermal stability, dynamic mechanical analysis, and flammability characteristics [14]. Moreover, different patterns of stacking the layers of laminate in cotton–bamboo fabric/glass fiber-epoxy composites proved that they had an effect on tensile, flexural, compressive and impact strength, and thermal properties [15]. Moreover, the composite was developed with synthetic fiber, which provided enhanced tensile and flexural strength and limited moisture absorption, resulting in better durability of the composite [16]. The glass fiber-epoxy composite was developed via a vacuum-assisted resin infusion production method, and the addition of the 1.5 wt% SiO_2 nanoparticles led to a higher tensile strength and modulus, higher hardness, and strengthened the fiber–matrix interfacial strength [17]. Indicatively, composites with kenaf fibers and polyamide 6 had varying thermal stabilities compared to pure polyamide 6 [18]. Treatment of silane-treated kenaf fibers with epoxy surface coating also enhanced thermal degradation and decompositional resistance of recycled poly (ethylene terephthalate) composites. On the same note, kenaf fibers that had been treated with resin coating improved the thermal properties of kenaf fiber/ABS polymer composites [19]. The epoxy composite laminate was developed with ramie/epoxy, Jute/epoxy, basalt/epoxy, and E-glass/epoxy via compression molding technique. The epoxy/basalt fiber laminate provided a higher tensile strength, improved flexural strength, and reduced moisture absorption [20]. Moreover, the composition of the polymer matrix composite and its optimized fabrication process parameters influenced the enhancement of the tensile strength, energy absorption, and thermal stability of the composite [21, 22]. The addition of the date seed granulated powder and carbon fiber leads to strengthening the interfacial action between the layers and provides higher mechanical properties of the composites [23]. The tensile strength behavior of the natural fiber-reinforced polymer matrix composite was studied, and Biopoxy 36 with 0.3 luffa fiber showed a higher tensile strength [24]. The natural luffa and palm fiber-reinforced high-density polyethylene thermoplastic laminates and chopped fiber provided higher mechanical properties and led to better analytical results [25]. However, the natural fiber-reinforced polymer composite showed better energy absorption and enhanced mechanical properties [26]. Furthermore, the additive manufacturing technique is suitable for mass production and is more expensive [27, 28].

Based on the previous studies, the epoxy composite developed with combinations of fiber laminates showed a higher tensile strength, lightweight, and improved fatigue strength. However, the epoxy matrix, having brittle and embedded with fiber laminates, found to have a poor interfacial strength and improved moisture absorption, reducing the overall functional properties of the composites. The novel silicon dioxide nanoparticles were used at different percentages for making epoxy composite laminates with different orientations of kenaf (KF), sisal (SF), and glass fiber (GF). Current research objectives are to prepare and enhance the functional properties of the epoxy hybrid composites, which consist of the kenaf/sisal/glass (KF/SF/GF) layers with different stacking and featuring SiO_2 nanoparticles via the hot compression mold technique. The contribution of SiO_2 nanoparticles and fiber stacking on mechanical and thermal characteristics was studied, and the resulting outcomes are compared. The research is intended to be conducted on the parameters of key performance, such as tensile and flexural performance, energy absorption capacity, thermal stability, and moisture absorption properties that are significant in structural applications subjected to mechanical load and changing environmental factors.

2 Materials and Methods

2.1 Materials

In this work, the reinforcements were kenaf (KF), sisal (SF), and E-glass (GF), provided by Green Materials, with an average fiber diameter of 50–100 μm for natural fibers and

15–20 μm for glass fibers. Diglycidyl ether of bisphenol-A (DGEBA) epoxy resin (Araldite LY 556) was used as an epoxy resin with a weight ratio of 10:1 mixed with an amine-based hardener (Aradur HY 951) [20]. The basic properties of the materials are shown in Table 1. To achieve a homogeneous dispersion of silicon dioxide SiO_2 nanoparticles with an average size of 50 nm, surface area 200 m^2/g, and without agglomeration, 3 wt% of nanoparticles was added to the epoxy matrix through ultrasonic agitation at 40 kHz for about 30 min, followed by high-shear mechanical mixing at 100 rpm for 30 min.

Here, the volume of the matrix and fiber are 50:50%, and the three layers were sequenced to kenaf (KF)/sisal (SF)/glass fiber (GF), and the thickness of each fiber is 1 ± 0.1 mm.

2.2 Preparation of Composite

The kenaf/sisal/glass (KF/SF/GF) hybrid epoxy laminates were prepared by the usage of the hot compression molding procedure, as it was chosen due to its capability to attain a high level of fiber volume fractions, and the epoxy resin was evenly applied throughout the fiber.

Fabrication was initiated by carefully mixing three separate fiber mat samples with KF, SF, and GF fiber mats to achieve homogeneous reinforcement of the hybrid in all samples. Four different stacking orders were developed to consider the effects of fiber orientation systematically: Sample 1 (KF/SF/GF at 0/0/0), Sample 2 (45/0/0), Sample 3 (0/45/0), and Sample 4 (0/0/45). Both configurations were made in two, one using a neat epoxy matrix and another one using 3 wt% SiO_2 nano-modified epoxy, to separate the multifactor influences. The epoxy resin and hardener were blended at a 100:10 ratio using a mechanical stirrer at 100 rpm. The required amount of nano-SiO_2 particles was added, and the stirring was continued for 10–20 min. Sequential lamination of the fiber mat pre-cut into 300×300 mm into a preheated steel mold kept at 80 °C for 10 min was the hand lay-up process used on each laminate. The process is shown in Fig. 1a, and a schematic diagram for laminate architecture and stacking sequence configurations is shown in Fig. 1b. Each fiber layer was coated very lightly with the epoxy resin plain and SiO_2_dispersed and allowed to dry under a vacuum of 0.1 bar with 10 min de-gasification to remove any trapped air [21]. The mold was subsequently closed, and the assembly placed in a hydraulic hot press at 120 °C platen temperature with the full load pressure of 5 MPa for 10 min, leading to strong bonding between the layers. Finally, the developed composite samples were kept in the die until reach room temperature (25 ± 1 °C at 60% RH). Edge trimming of laminates followed post-demolding to 290×290 mm $\times 10$ mm. Finally, the thickness of plates was evaluated at ten different places using a digital micrometer with an accuracy of ± 0.001 mm, and the average value was confirmed to demonstrate the repeatability of the measurements.

2.3 Test Specification

The microstructure of the developed composites was analyzed by using a high-resolution TESCAN-VEGA3 scanning electron microscope. Before the analysis, the sample was prepared to a 10 mm $\times$ 10 mm $\times$ 10 mm glass-polished surface. Tensile properties, yield strength, ultimate strength, elongation at break, and Young's modulus are determined based on ASTM D3039 [29, 30] of polymer matrix composite laminates, where the specimen is a straight side coupon; length about 250 mm and width about 25 mm, and the laminate thickness about 3 mm acts as the depth of the specimen, a gauge length of 150 mm, and bonded glass/epoxy end tabs about 50 mm. Flexural strength and flexural energy absorption are determined through three-point bending tests to ASTM D790, using rectangular-shaped specimens approximately 127 mm long, 12.7 mm wide, and using a thickness equal to the laminate, a span is placed on the specimen to be 16 times the thickness of the laminate (span-to-depth ratio of 16:1), and the maximum flexural stress is determined by evaluating the maximum load, and the energy absorbed is determined by evaluating the area under the flexural load deflection. According to ASTM D6110, the Charpy impact strength of the epoxy composite laminates was evaluated by using an Instron make CEAST 9000 series equipped with a 50 J pendulum and having 3.8 m/s impact velocity. A minimum of three samples from each epoxy composite laminate was evaluated and the average impact strength together with the 5% standard deviation. ASTM D570 is

Table 1 Properties of the materials

Material	Type/role	Density (g/cm^3)	Tensile strength (MPa)	Young's modulus (GPa)
Sisal fiber	Natural lignocellulosic fiber reinforcement	1.3–1.5	400–700 (single fiber)	9–22
Glass fiber (E-glass)	Synthetic high-strength fiber reinforcement	2.5–2.6	1900–3400	70–80
Kenaf fiber	Natural bast fiber reinforcement	1.2–1.4	283–800 (single fiber)	20–35
Silica nanoparticles (SiO_2)	Inorganic nanofiller/matrix and interphase reinforcement	2.2	Strength given via composite, not bulk	70–75 (bulk silica

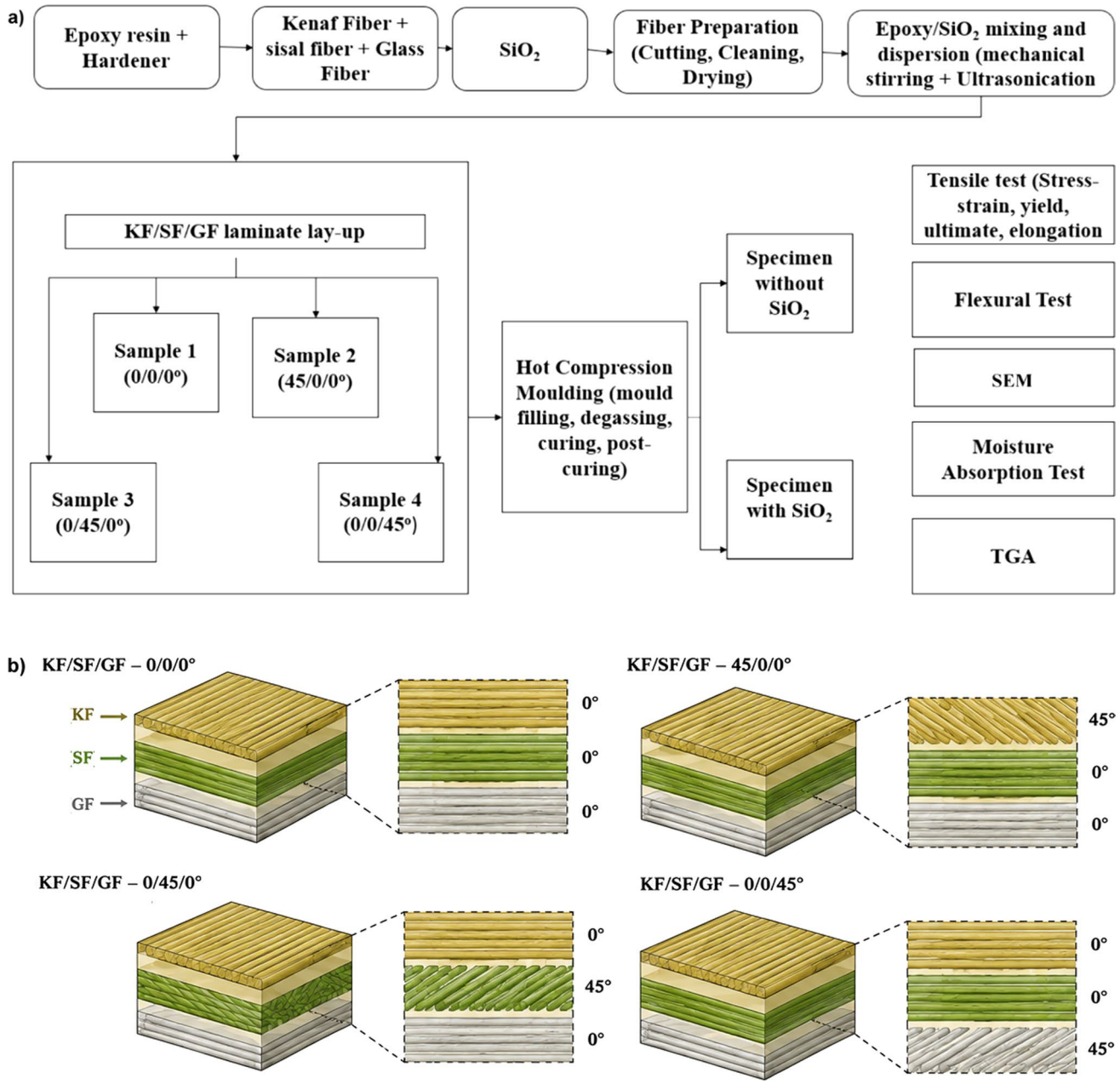

Fig. 1 **a** Process Flow of the Fabrication Process, **b** schematic diagram for laminate architecture and stacking sequence configurations

used to assess more moisture absorption behavior with the laminate strips of approximately 76 × 25 × 3 mm dried and conditioned at constant mass then immersed in distilled water usually at a constant temperature of 23 °C at specified intervals; the specimen is periodically removed, dried at 105 °C, weighed, and the percent weight gain of the specimen versus the duration of immersion is plotted to determine the moisture uptake of both SiO_2_ filled and unfilled hybrids. Before testing, each composite specimen was divided into three test samples to confirm the reliability and repeatability of the mechanical testing, and the average value was used for discussion with a 5% significance level. Thermogravimetric TGA is based on ASTM E1131 to measure both compositional and thermal stability, where a small sample 5–20 mg of the laminate is cut and used in powder form or cut into a small sample used in a thermal decomposition reaction, and the data collected are the mass-loss curves of the material; both as a function of temperature which reveal decomposition temperatures, residual char, and inorganic content that could help determine the influence of the addition of SiO_2 nanoparticles to the composite on thermal behavior.

3 Results and Discussion

3.1 Microstructure Analysis

Figure 2a–d and e–h shows the cross-sectional SEM images of the epoxy hybrid laminates without and with 3 wt% SiO_2 nanoparticles.

The SEM image of Sample 1 w/o SiO_2 nanoparticles (KF/SF/GF-0/0/0 degree) is shown in Fig. 2a. The applied epoxy and effective compression pressure lead to strong bonding between the fibers. Figure 2 shows the SEM image of the epoxy composite laminate Sample 2 prepared by 45/0/0 degrees of the KF/SF/GF layer and the epoxy layer, identified as a thin layer and cross-section, where KF was dispersed in the epoxy matrix under applied compression pressure. This leads to resisting fiber dislocation and may cause changes to slide the SF and GF during higher tensile load due to unidirectional [2, 3]. The SEM images of Sample 3 (0/45/0 degree of KF/SF/GF) and Sample 4 (0/0/45 degree of KF/SF/GF) are shown in Fig. 2c-d. However, a uniform compression force leads to strong adhesion behavior, and the intermediate 45-degree SF fiber forms a strong interface between KF/GF, resulting in higher stress concentration and limiting fiber displacement, thereby increasing tensile strength.

The SEM images of the epoxy composite laminates developed with 3 wt% SiO_2 nanoparticles are shown in Fig. 2e–h, and Sample 1 with 3 wt% SiO_2 nanoparticles is shown in Fig. 2e. The presence of the nanofiller is confirmed via SEM image and strongly dispersed within the fiber layer, leading to higher stress concentration. Sample 2 with 3 wt% SiO_2 nanoparticles (45/0/0 degrees KF/SF/GF with nanofiller) is shown in Fig. 2f, and the nano-SiO_2 nanoparticles are strongly dispersed in a wide area of the intermediate epoxy layer, which supports an effective pinning action between the layers, resulting in enhanced energy absorption [6]. The SEM image of Sample 3 (0/45/0 degrees KF/SF/GF with nanofiller) shows an effective interaction with the fibers (Fig. 2g) and leads to a mechanism for higher load-carrying capacity, resulting in enhanced mechanical properties of the composite. The SEM image of Sample 4 (0/0/45 degrees KF/SF/GF with nanofiller) is illustrated in Fig. 2h. However, the nano-SiO_2 particle strengthens the bonding and provides a strong pinning action mechanism to resist the dislocation of the fiber.

3.2 Tensile Strength Performance

Sample 3 has the best overall tensile response, including the highest yield strength of 52 MPa, ultimate tensile strength of 72 MPa is shown in Table 2, elongation at break 4.1%, and Young's modulus of 3200 MPa in the unfilled state. It means that by putting the off-axis (45°) lamina in the center, the transfer of shear is improved, and interlaminar damage is delayed such that the laminate itself can sustain a higher load without losing its good deformability [8, 12]. In Sample 1 (0/0/0°), all plies are oriented, resulting in the load being mainly handled in the fiber direction; this has the advantage of causing the laminate to be stiff, but it is more susceptible to fiber breakage and matrix cracking when the critical stress is reached, with an ultimate strength of 65 MPa and elongation of 3.2%.

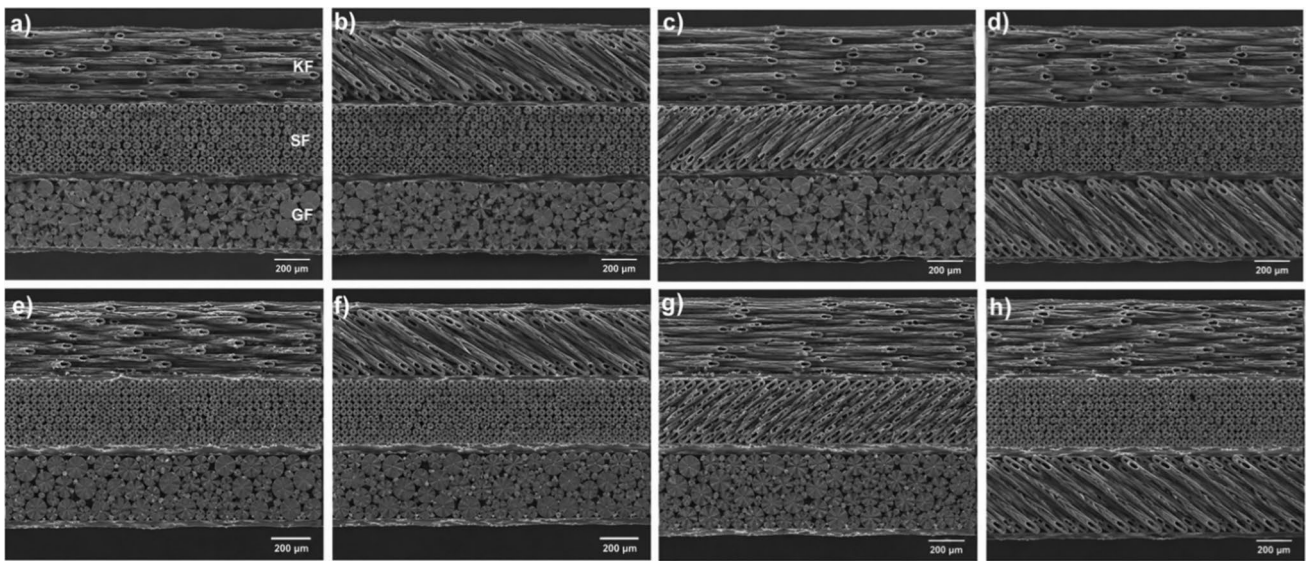

Fig. 2 SEM images of the **a** Sample 1 w/o SiO_2, **b** Sample 2 w/o SiO_2, **c** Sample 3 w/o SiO_2, **d** Sample 4 w/o SiO_2, **e** Sample 1 w SiO_2, **f** Sample 2 w SiO_2, **g** Sample 3 w SiO_2, and **h** Sample 4 w SiO_2

Table 2 Tensile properties of composites

Notation	Sample	Yield Strength (MPa) w/o SiO_2	Ultimate Strength (MPa) w/o SiO_2	Elongation (%) w/o SiO_2	Young's Modulus (MPa) w/o SiO_2	Yield Strength (MPa) w/3% SiO_2	Ultimate Strength (MPa) w/3% SiO_2	Elongation (%) w/3% SiO_2	Young's Modulus (MPa) w/3% SiO_2
1	KF/SF/GF-0/0/0°	45	65	3.2	2800	51.7	76.7	3.04	3416
2	KF/SF/GF-45/0/0°	48	68	2.8	2950	53.8	78.2	2.58	3540
3	KF/SF/GF-0/45/0°	52	72	4.1	3200	65	92.2	4.3	4160
4	KF/SF/GF-0/0/45°	47	67	3	2850	55.5	80.4	2.82	3506

Sample 2 (45/0/0) and Sample 4 (0/0/45) incorporate asymmetry in the lay-up, where only one off-axis ply forms the outer surface, resulting in moderate gains in load redistribution but initiating interfacial debonding and matrix cracking significantly earlier than the balanced 0/45/0 structure. Small modulus values of the Young 2950 MPa and 2850 MPa, respectively, show that without the reinforcement on the nanoscale, the stiffness is highly controlled by the fraction of glass fibers [22]. The addition of SiO_2 nanoparticles results in a steady increase in tensile behavior of all stacking orders, and Sample 3 demonstrates the greatest increase. The yield strength, ultimate strength, and Young's modulus of the 0/45/0-degree laminate are increasing to 52, 72, and 92.2 MPa, respectively, and the modulus of elasticity increases to 4160 MPa. These increments are normal in epoxy hybrids, which contain well-dispersed SiO_2, where the nanoparticles become the stiff stress-bearing locations, the crack-deflecting locations at the interface of the matrix/particle, and the strengthening of the fiber/matrix interface by reducing microvoids, the microstructure of the SiO_2_dispersed sample as shown in Fig. 2e–h. The small effect on elongation, 4.1%–4.3% in the sample, indicates that the better interface bonding and more uniform distribution of stress postpone catastrophic coalescence of the cracks; hence, the laminate is able to deform slightly more before failure in spite of its increased strength. In Samples 1, 2, and 4, the strengthening and modulus of the material are also increased by SiO_2; however, the increase in ductility is less, and in certain instances, the elongation diminishes slightly. As Sample 1 shows, a yield and ultimate strength increase of 45–51.7 MPa and 65–76.7 MPa, and Young's modulus rises by 2800–3416 MPa, with only a slight decrease in elongation of 3.2–3.04.

In the absence of SiO_2, all four laminates have an initially steep, near-linear behavior to approximately 0.3%–0.5% strain, which corresponds to elastic loading of the glass and aligned natural fibers. The peak stress in Sample 3 (0/45/0) is the highest, and the strain at the peak is slightly higher, which corresponds to its better yield and ultimate tensile strengths, 52 MPa and 72 MPa shown in Fig. 3a and the largest elongation, 4.1%. The 45° ply in the core layer is beneficial as it encourages effective transfer of shear between adjacent plies and also slows the initiation of interlaminar cracking, providing this laminate with an extended plateau area and slower post-maximum stress softening. Sample 1 (0/0/0), on the other hand, stabilizes stress faster, having less of a peak and a shorter plastic regime, indicating previous fiber breakage and matrix splitting as all the plies are oriented in the same direction [11]. Samples 2 (45/0/0) and 4 (0/0/45) are intermediate between these two extremes with moderate maxima and post-peak responses, which indicate asymmetric lay-ups in which only one of the off-axis plies engages in shear redistribution. Sample 3 containing SiO_2 has the highest level of stress, as compared to all other curves; it indicates the synergistic performance of a well-optimized architecture of 0/45/0 and a stiffened epoxy matrix enhanced with well-dispersed SiO_2 and its microstructure is shown in Fig. 2g. The nanoparticles serve as micro-stress carriers, decrease microvoids, and enhance the fiber/matrix interphase, and thus, the laminate maintains more loads before the unstable cracking starts. The post-peak deceleration of SiO_2_filled Sample 3 is slow, which means that nano-toughening postpones disastrous delamination and fiber pull-out. In the case of Samples 1, 2, and 4, SiO_2 also increases the stress plateaus and peak values. However, the softening region is slightly sharper, which is also in accordance with a more rigid matrix, which initiates crack localization at a faster rate upon critical damage localization [15]. The separate w/o SiO_2 and w SiO_2 indicate that in all the stacking sequences, the incorporation of nanoparticles is always beneficial in tensile load-bearing capacity, and the maximum advantage is achieved in Sample 3, which proves to be the best configuration of each stacking sequence in structural performance.

Based on the findings, the Sample 3 epoxy composite laminates (KF/SF/GF with 3 wt% SiO_2) showed a higher

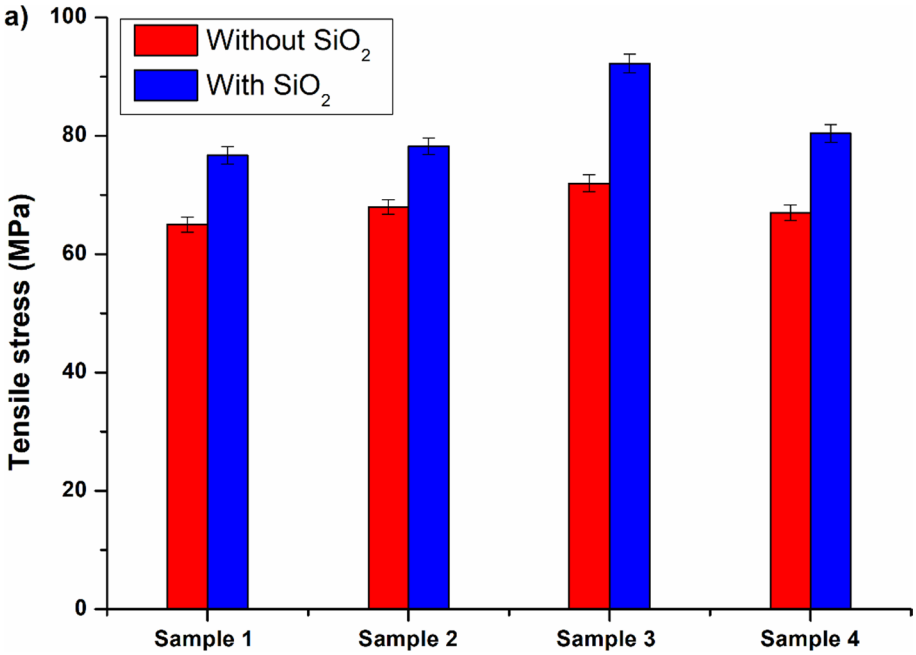

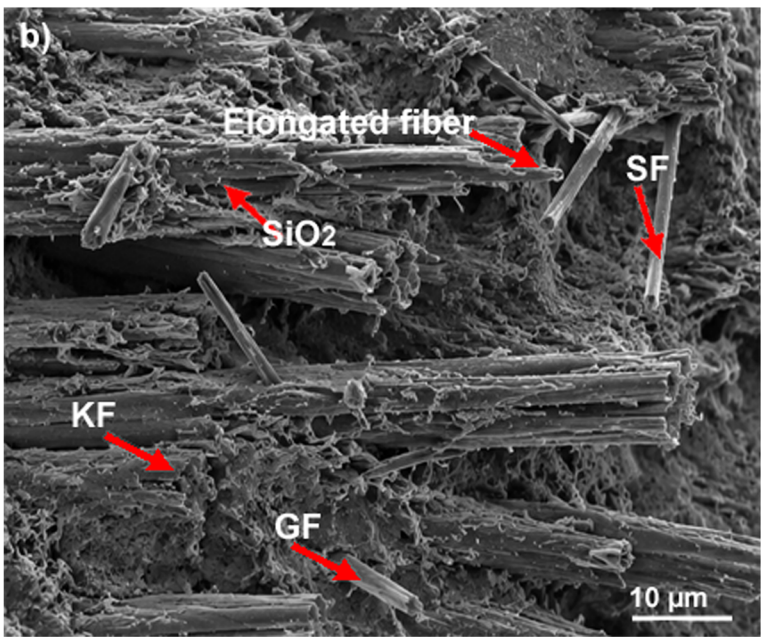

Fig. 3 **a** Tensile strength of the epoxy composite laminates without and with SiO_2, **b** fractography surface of tensile fracture of Sample 3 epoxy composite laminates (KF/SF/GF with 3 wt% SiO_2)

tensile strength performance than the others. So, the fractography surface of tensile fracture of Sample 3 epoxy composite laminates (KF/SF/GF with 3 wt% SiO_2) is shown in Fig. 3b. The 45-degree dispersed SF, along with strong SiO_2 dispersion, leads to a higher load-carrying capacity and results in an elongated fiber failure. An effective compression action and even dispersion of the nanofiller between the fibers lead to resisting the dislocation of the fiber and enduring a maximum stress concentration, resulting in enhanced tensile strength. The KF and GF are strongly dispersed into the epoxy matrix and provide a higher adhesion behavior. The nanofiller limits the crack propagation.

3.3 Flexural Strength

Sample 1 forms a flexural strength higher than 95 MPa without the addition of SiO_2, and even then, it is the lowest of all four laminates, but still comparable to other normal kenaf/glass–epoxy systems. The 0/0/0 lay-up is fully unidirectional with tensile and compressive stresses to the fiber axis on the outer plies in the bending action. Without

nanofiller, the epoxy matrix has its original toughness and stiffness, thus microcracks born at fiber–matrix boundaries can easily form due to flexural loading. In the case of SiO_2, flexural strength increases to 120 MPa, which is a 26% improvement. This is in line with the reports that dispersing SiO_2 in epoxy leads to fewer microvoids, higher local stiffness, and crack path tortuosity; more energy is needed to propagate flexural cracks. In Sample 2, flexural strength without SiO_2 is 100 MPa, which is a little higher in comparison with Sample 1 because a 45 ply is introduced.

The top surface of the off-axis lamina helps in transferring shear loads and minimizing the stress concentration in the matrix by redistributing to in-plane shear in the ply [3, 6]. This arrangement can increase interlaminar shear resistance and delay delamination between the outer and inner ply more than a fully 0-degree stack. Nevertheless, due to the fact that there is only one off-axis ply, the enhancement is moderate [23]. When SiO_2 is added to it, the flexural strength increases again to 125 MPa, about 25% shown in Fig. 4a. The inclusion of SiO_2 lowers the dimensions and rate of propagation of matrix cracks commencing about

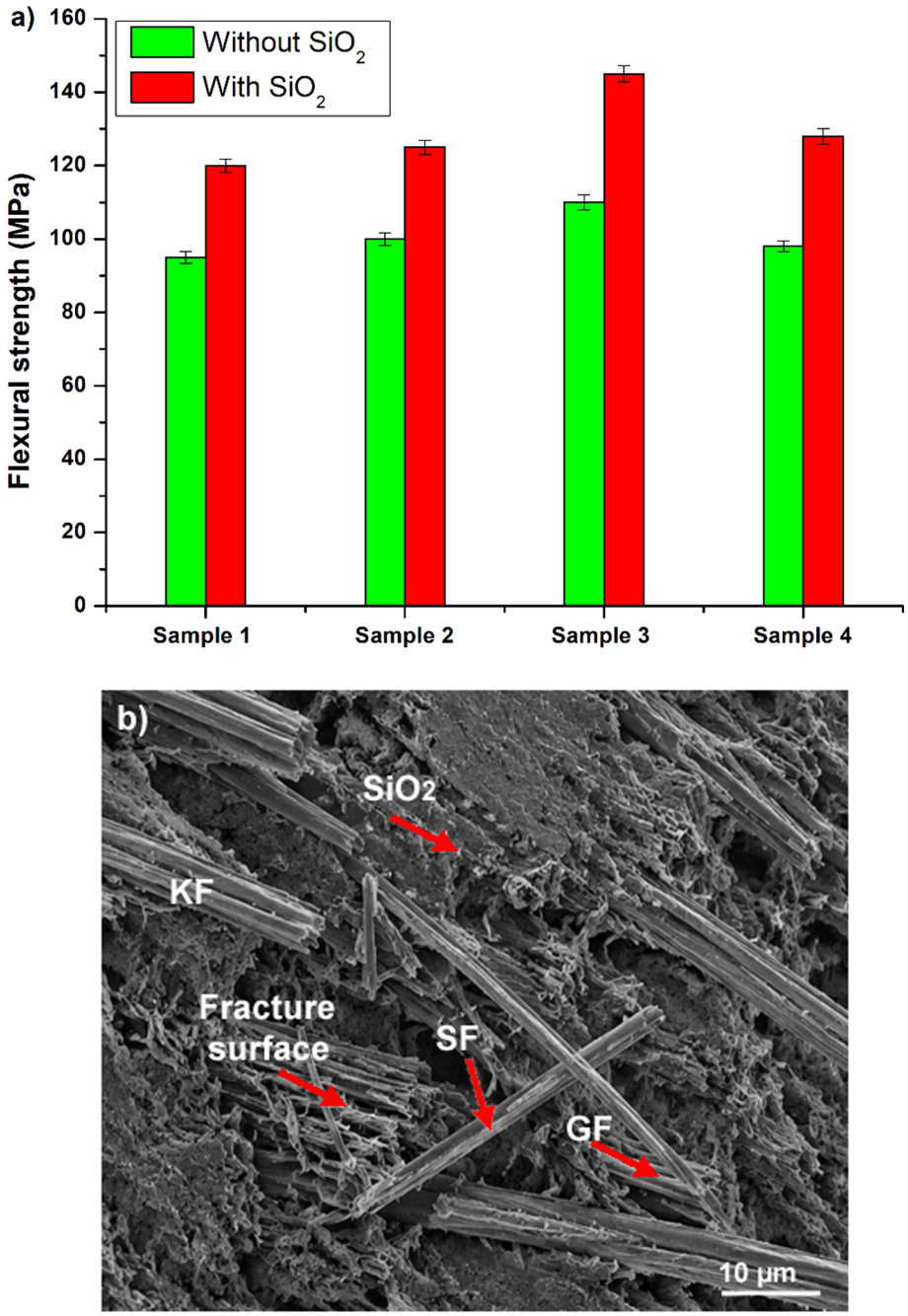

Fig. 4 **a** Flexural strength of epoxy composite laminates without and with SiO_2, **b** fractography surface of flexural strength of Sample 3 epoxy composite laminates (KF/SF/GF with 3 wt% SiO_2)

the compressed 45-degree ply and tensile 0-degree ply and extending the quasi-linear period of the flexural stress–strain reaction and raising the utmost weight. In general, Sample 2 containing SiO_2 demonstrates a balanced response in which fiber orientation and nanoparticle reinforcement are used to enhance bending capacity. Sample 3 performs the highest flexural strength of 110 MPa without SiO_2. The 0/45/0 lay-up is symmetrical, whereby the 45 ply is in the mid-plane, which is the location of maximum interlaminar shear during three-point bending. This structure is effective in bridging tensile and compressive faces, and shear stress is reallocated using the off-axis fiber and delamination and matrix crack propagation at the neutral axis is delayed. With the addition of SiO_2, the flexural strength goes up by a significant amount, approximately 145 MPa, about 32% higher, which is on the higher side of the improvement that has been reported in optimum filled epoxy/SiO_2 hybrids. In this optimum structure, the SiO_2 are widely distributed with in the matrix, Specifically across the high shear mid-plane in the surrounding the tensile/compressive fibers [5, 29].

The 45 ply in Sample 4 is moved to the lower surface, thereby making the laminate asymmetric. The flexural strength without SiO_2 is 98 MPa, which is marginally higher than that of others. With the addition of SiO_2, the flexural strength is brought up to 128 MPa, which is an increase of approximately 30%. The SiO_2 makes the matrix stiffer and stronger on tensile and compressive sides; hence, although the stacking sequence is not optimally oriented, the laminate is capable of supporting considerably higher bending moments. The reinforced network structure surrounding the 45-degree fibers of the bottom ply enhances resistance to shear-induced splitting. In contrast, the outer 0-degree plies enjoy the advantage of a more resistant and resistant to crack propagation, higher resin richness, and presence of the nano-filler, which resists the fiber movement and provides better interface strength, resulting in enhanced flexural strength of the composite [11].

Figure 4b shows the fractography surface of the flexural strength of Sample 3 epoxy composite laminates (KF/SF/GF with 3 wt% SiO_2). The presence of the nano-SiO_2 particles between the fiber matrixes acts as a crack bridging and enhances the adhesive bonding strength, resulting in an enhanced load-carrying capacity and limits the crack initiation. The combined actions of the KF/SF/GF layer with 0/45/0 stacking with nanofiller endure a maximum load and lead to higher flexural strength of the composite, and the failure fracture surface is shown in Fig. 4b.

3.4 Impact Strength

The improvement in the impact strength data indicates that the addition of SiO_2 leads to a systematic increase in the values of all laminates, with Sample 3 recording the highest values under both conditions. In the absence of SiO_2, the impact strength reduces to 18 kJ/m^2 in Sample 1 and 23 kJ/m^2 in Sample 3, and this shows that fiber sequencing and off-axis plies have a strong influence on impact energy absorption. With a completely 0 degrees laminate sample 1, deformation is predominantly in the fiber direction. Therefore, once a crack sets up at the tensile face, it spreads quickly through fiber interfaces, leading to a low amount of energy being absorbed before fracture.

The addition of 45 plies in Samples 2, 3, and 4 introduces the capability of supporting shear deformation, and enhancing fiber pull-out and matrix shearing, enhancing work of fracture. Sample 3 with a balanced configuration is the most effective as the intermediate ply of 45 is placed in the proximity of the neutral axis, where interlaminar shear is greatest, as shown in Fig. 5a. This structure increases crack deflection paths along the laminate thickness and makes cracks run around fibers of varying orientations, increasing both the tortuousness of crack paths and energy dissipation. The fact that Sample 4 has a slight decrease compared to Sample 3 implies that an asymmetric lay-up cannot redistribute impact-induced stresses to the same extent that a symmetric sequence does.

In SiO_2, the impact strength increases in each of the four samples, 24, 27, 31, and 26 kJ/m^2, respectively, which demonstrates the effect of SiO_2 on increasing the toughness and stiffening tendency in the epoxy matrix and fiber/matrix interface. The dispersed SiO_2 particles can serve as crack arresters and deflection sites. Impact-driven crack front bouncing against a rigid nanoparticle causes stress fields locally, which cause the crack to branch/deflect/to form microcracks around the particle rather than running straight through. This enhances the area of the fracture surface and the energy needed to propagate cracks and consequently raises impact resistance. Moreover, SiO_2 decreases microvoid content and enhances the interphase by offering an extra mechanical bond and perhaps hydrogen bonding with hydroxyl groups on kenaf and sisal fibers, and thus, fiber debonding and pull-out require more energy [24]. Sample 3 has the highest relative increase in impact strength of 23–31 kJ/m^2. This suggests that there exists a high synergy between optimized 0/45/0 fiber structure and a nano-reinforced matrix. The 45-degree mid-ply gives a series of shear and deflection planes, whereas the harder SiO_2-reinforced epoxy postpones matrix crackage and stabilizes interlaminar shear transfer. Samples 1, 2, and 4 show a smaller but still significant improvement in impact strength, which confirms that SiO_2 nanofillers are effective regardless of the lay-up, but must have the greatest effect when fiber sequencing already favors progressive damage and crack deflection, such as in the 0/45/0° laminate.

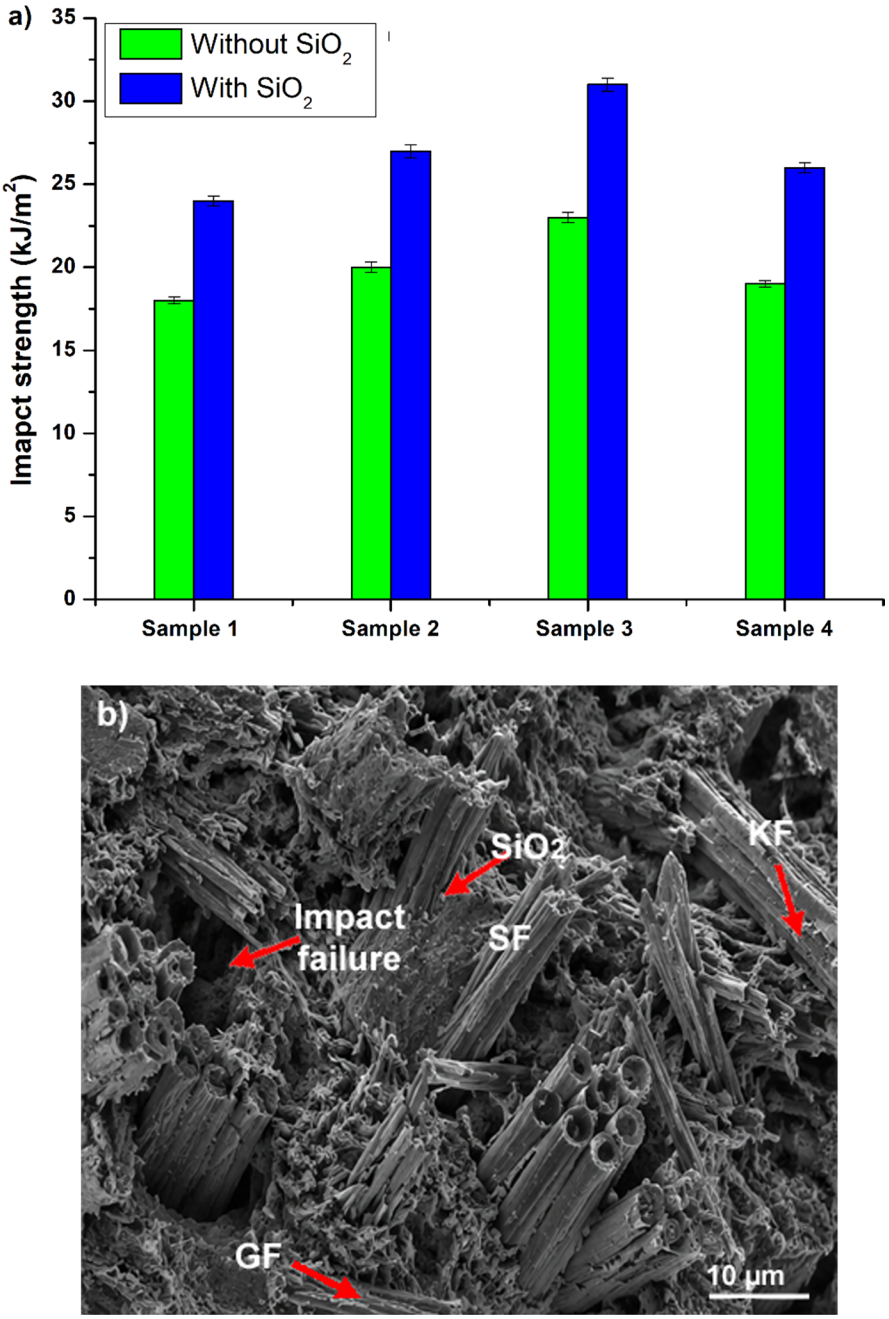

Fig. 5 **a** Impact strength of epoxy composite laminates without and with SiO_2, **b** fractography surface of impact fracture of Sample 3 epoxy composite laminates (KF/SF/GF with 3 wt% SiO_2)

Figure 5b shows the impact failure surface of the epoxy composite laminates Sample 3 (KF/SF/GF with 3 wt% SiO_2). The additions of the nano-SiO_2 particles provide a crack bridging and enhance the bonding interface between the fibers, resulting in a mechanism for an effective fiber–matrix pinning, which leads to higher energy absorption. A higher impact load is required to break the epoxy layer, and the fiber is crushed, and the impact failure zone is highlighted in Fig. 5b. However, the 45-degree SF with strong dispersion of nanofiller absorbs the impact energy and enhances the composite's impact strength.

3.5 Moisture Absorption

Figure 6 shows the water absorption behavior of the epoxy composite laminates. The water absorption data evidently reveal that each of the four KF/SF/GF laminates acquires less moisture in the presence of SiO_2 nanoparticles, where Sample 3 takes the least amount of moisture in both circumstances. In the absence of SiO_2, the diffusion level at four samples, 1–4, is 4.2, 3.9, 3.5, to 4.0%, respectively, which is a combination of natural fiber content, fiber orientation, and laminate symmetry that influences diffusion paths and void structure. The kenaf and sisal fibers in such hybrids

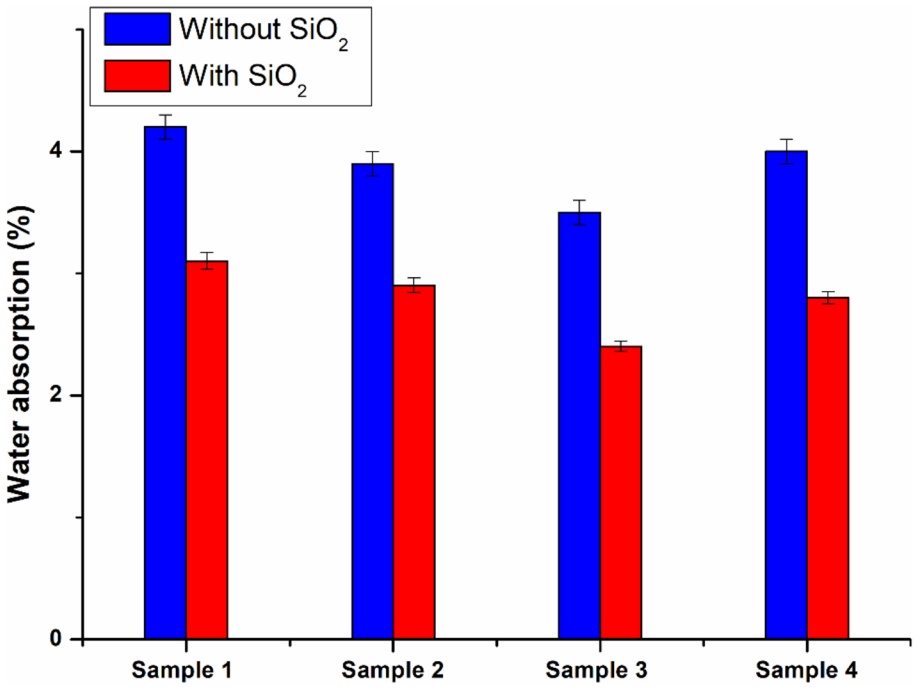

Fig. 6 Moisture absorption of epoxy composite laminates without and with SiO_2% composites

are extremely hydrophilic with their cellulose, hemicellulose, and lumen pores, such that the water molecules mainly penetrate along fiber lumens, interfibrillar microvoids, and between imperfect fiber interfaces.

The best consolidation and distribution of stress during hot compression is offered by Sample 3, which can minimize residual voids and enhance impregnation of the fibers by the epoxy, thus slightly lowering the equilibrium uptake compared to the more unidirectional and asymmetric lay-ups. The microstructure of Sample 3 developed with 3 wt% SiO_2 nanoparticles is shown in Fig. 2g. Sample 1, which has all of the plies at 0, and Sample 4, which only has the 45-degree ply on one side, have more of the microgaps and resin-lean areas around the natural fibers, providing easier avenues for water and, therefore, higher percentages of absorption [3, 9]. On addition of SiO_2, the water uptake of each laminate decreases drastically to 3.1, 2.9, 2.4, and 2.8% in Samples 1–4, respectively, as shown in Fig. 6 and an improvement of 31%. This reduction is in agreement with documented behavior of SiO_2_modified epoxy and natural fiber composites, with nanoparticles serving as micro-fillers, which fill the free-volume, densify, and seal microvoids at the fiber interface. Moreover, the microstructural compactness and presence of the nano-SiO_2 nanoparticles could strongly interface with the fiber, resulting in a higher moisture absorption resistance, and the samples developed with 3 wt% nano-SiO_2 nanoparticles showed a better moisture absorption resistance compared to the sample developed without nano-SiO_2 nanoparticles. The microstructure compactness is shown in Fig. 2e–h. The SiO_2 suppresses the diffusion process and reduces the final equilibrium moisture content by physically blocking channels of diffusion to form a more tortuous path. Also, SiO_2 surfaces may react with the epoxy and the number of hydroxyl groups on the fibers, enhancing the bond between interfaces, and more adhesive interfaces make the bond resistant to debonding in hygroscopic swelling, which would, otherwise, create new diffusion paths. Sample 3 with SiO_2 is the most water resistant with a minimum water uptake of 2.4%, suggesting that there is a very strong synergy between a 0/45/0° stacking sequence, which is optimized and the densification of the matrix induced by nanofillers [25]. The uniformity of pressure and flow of resin during hot compression is more uniform in the symmetric lay-up, thus SiO_2 disperses better and fills micro-defects throughout the laminate thickness more effectively. Sample 3 containing SiO_2 has the smallest microstructure, and the least interconnected network of voids and strong interface bonding is shown in Fig. 2g, and this is the reason why it simultaneously exhibits the highest mechanical properties and lowest absorption of moisture when compared to the other laminates.

3.6 Thermogravimetric Analysis

The four kenaf/sisal/glass–epoxy laminates, in the absence of SiO_2, show the common three-stage degradation behavior of natural fiber polymer composites, with Sample 3 thermally the most resilient. All these samples exhibit a minor increase in weight loss, mainly by evaporation of physically absorbed moisture and desorption of the low-molecular-weight species of the hydrophilic kenaf and sisal fibers at

low temperatures up to around 200 °C which are shown in Fig. 7a.

The curves nearly coincide in this region, showing that the orientation of fibers does not significantly affect the process of removing bound water. At temperatures between 250 and 350 °C, the rate of weight loss begins to increase as the hemicellulose and less resistant components of the epoxy matrix decompose. A significant reduction occurs between about 320 and 450 °C associated with the simultaneous degradation of cellulose, lignin, and the crosslinked network of epoxy. These slight leftwards or rightwards movements of this major transition represent the effectiveness with which the hybrid architecture allocates heat and copes with stresses caused by decomposition. Sample 3 continually exhibits a marginally slower onset of rapid weight reduction and reduced terminal weight loss at high temperature

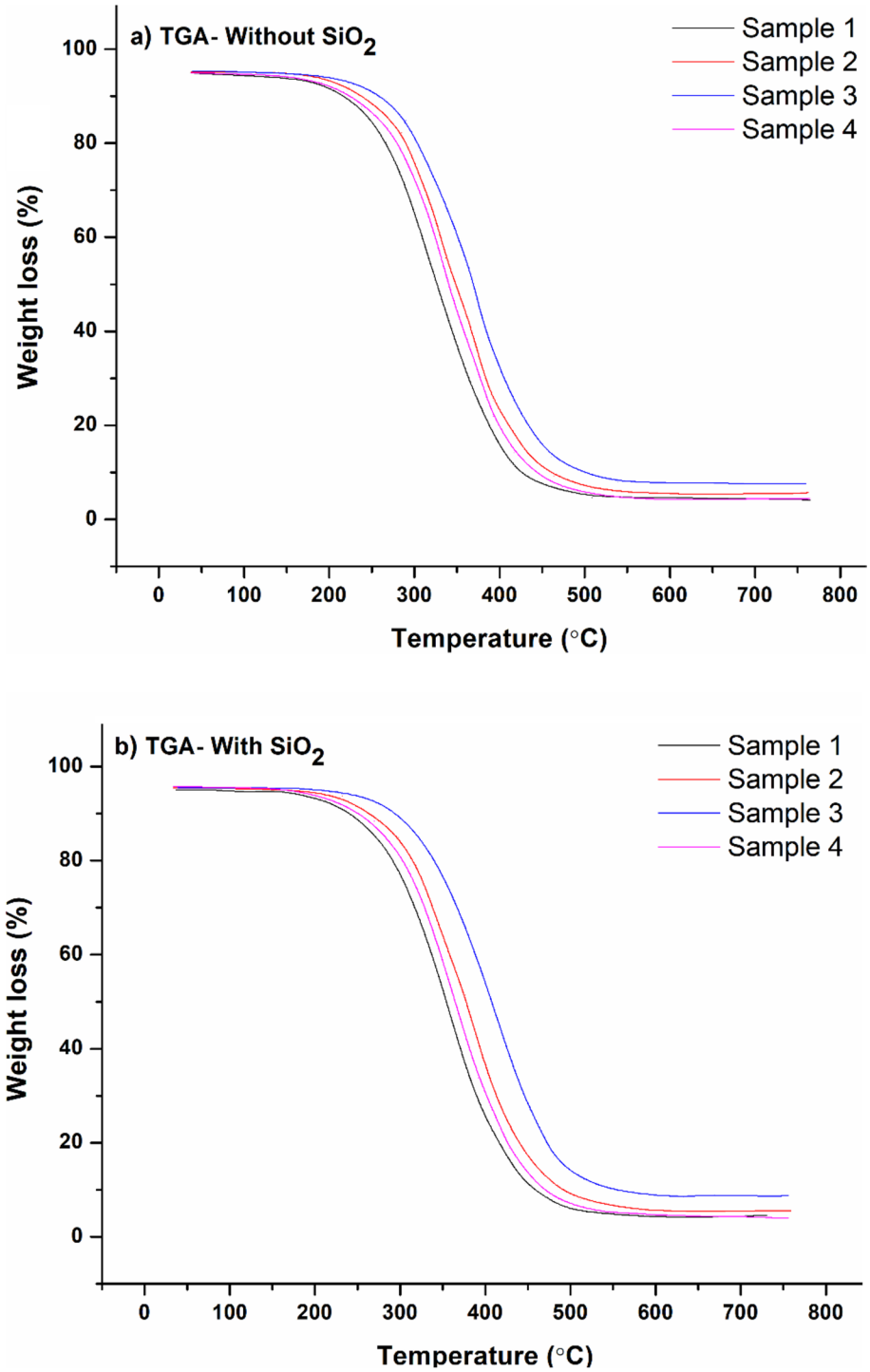

Fig. 7 TGA curve (**a**) without SiO_2 and **b** with SiO_2

than Samples 1, 2, and 4, that is, increased char residue and a greater thermal stability. It is possible to associate this behavior with the symmetric lay-up, which positions the 45° ply at the mid-plane where interlaminar shear stresses are greatest during heating. Such an arrangement facilitates the reduction of non-uniform stress and fiber packing, which lessens the density of microvoids and interfacial flaws, which serve as favored hot spots of thermal cracking and hot volatile escape. In comparison, the fully unidirectional asymmetric laminates probably have more resin-rich areas and fewer constrained natural fibers to cause degradation and leave less carbon residue. Accordingly, Sample 3 sequencing is the most thermally stable architecture of the read-out laminates tested.

The TGA weight loss profiles of the SiO_2-filled KF/SF/GF laminates reveal that incorporation of SiO_2 improves the thermal stability of all the stacking sequences, with Sample 3 performing the most desirable behavior. At low temperatures up to approximately 200 °C, the four curves nearly overlap and exhibit a minimal loss of weight corresponding to the desorption of the physically absorbed moisture and the extraction of low-molecular-weight volatile substances in the fibers and epoxy. The SiO_2 concentration does not have a big role in this step, which means that the hydrophilic kenaf and sisal stages control moisture desorption. Temperature rise to 250–350 °C slightly increases, as shown in Fig. 7b, the onset of rapid weight loss by SiO_2-filled laminates relative to unfilled laminates, which is an indication of the stabilizing effect of SiO_2 on the lignocellulosic components and epoxy network. The primary decomposition phase at approximately 330–460 °C still exists. Still, its slope is steeper, and its residual mass at higher temperatures is greater in all of the samples, indicating better char formation and less overall degradation. Sample 3 is the least weight loss and the heaviest residual mass across the SiO_2 laminates, which supports the conclusion that the 0/45/0 laminates are the most thermally resistant when reinforced with nanoparticles [2, 26]. The ply in the middle at 45 degrees, with reference to the neutral axis, allows equal distribution of stress and heat and offers numerous tortuous routes and escape routes for the gases to degrade. This architecture is more preferential when SiO_2 exists, which is more effective in dispersing nanoparticles and filling the microvoids at the interface of the fiber, leading to a denser and more thermally resistant structure. On comparing the curves of the presence and absence of the SiO_2 in all the samples, the two overall trends, namely, the SiO_2-modified laminates, exhibit a slow decomposition and high char yield and that the same is more prevalent in Sample 3. This implies that matrix nano-reinforcement and fiber sequencing are significant. Still, their interaction is optimized in the symmetric 0/45/0-degree geometry, hence offering the most efficient thermal behavior of the hybrid composites. Table 3 shows the stages of degradation temperature and char residue at 750 °C.

Based on the investigation findings, the epoxy composite laminate Sample 3 (0/45/0) showed a higher performance than the others, which is compared to the previous research and shown in Table 4.

The significance of a 3 wt% SiO interfaced epoxy hybrid composite laminate with 0/45/0 degree of KF/SF/GF (Sample 3) showed a higher tensile strength, flexural strength, and impact strength than the other samples. The tensile strength of the Sample 3 is 48.9%, 1.2%, and 137.6% higher than the epoxy hybrid composite laminate was prepared by using a jute/sisal fiber embedded in an intralaminar orientation of E-glass fiber via wet filament winding process [2], epoxy hybrid composite laminate was prepared by using a jute/kenaf/glass fiber with 5 wt% graphene via hand layup associated with the compression molding process [9], hybrid biocomposite was developed by using a 20 wt% kenaf fiber via the compression molding process [12]. Similarly, the flexural strength of Sample 3 composite is 72.8%, 83.7%, and 57.11% higher than the epoxy hybrid composite laminate was prepared by using a jute/sisal fiber embedded in an intralaminar orientation of E-glass fiber [2], the hybrid biocomposite was developed by using a 20 wt% kenaf fiber [12]], and the ramie/jute/Unsaturated Isophthalic Resin (UIR) and epoxy resin laminates [20]. However, the energy

Table 3 Stages of degradation, temperature, and char residue at 750ºC

Samples	Initial degradation stage- $T_{5\%}$ (°C)	Onset decomposition temperature- T_{onset} (°C)	Maximum degradation temperature—T_{max} (°C)	Char residue at 750 °C (%)
Sample 1 (W/O-3 wt% SiO_2)	202	306	362	17.8
Sample 2 (W/O-3 wt% SiO_2)	203	309	365	18.6
Sample 3 (W/O-3 wt% SiO_2)	205	317	371	21.8
Sample 4 (W/O-3 wt% SiO_2)	204	312	367	20.8
Sample 1 (With-3 wt% SiO_2)	204	322	375	16.5
Sample 2 (With-3 wt% SiO_2)	206	326	378	17.6
Sample 3 (With-3 wt% SiO_2)	208	331	382	19.5
Sample 4 (With-3 wt% SiO_2)	208	329	379	19.3

Table 4 Novelty comparison of the present research to the previous studies

Details of the composites	Tensile strength in MPa	Flexural strength in MPa	Impact strength in kJ/m^2	References
The epoxy hybrid composite laminate with 0/45/0 degrees of KF/SF/GF with 3 wt% of SiO_2 via hot compression molding production method	92.2	145	31	Present research
The epoxy hybrid composite laminate was prepared by using a jute/sisal fiber embedded in an intralaminar orientation of E-glass fiber via a wet filament winding process	61.91	83.9	–	[2]
The epoxy hybrid composite laminate was prepared by using a jute/kenaf/glass fiber with 5 wt% graphene via hand lay-up associated with the compression molding process	91	–	–	[9]
The hybrid biocomposite was developed by using a 20 wt% kenaf fiber via the compression molding process	38.8	78.9	1.8	[12]
The ramie/jute/unsaturated Isophthalic Resin (UIR) and epoxy resin laminates were prepared via the compression molding technique	–	92.29	–	[20]

absorption of the epoxy hybrid composite laminate with 0/45/0 degree of KF/SF/GF with 3 wt% of SiO_2 showed more than 100% better than the hybrid biocomposite developed with 20 wt% kenaf fiber [12].

- However, this study is limited by adding a SiO_2 content not more than 3 wt%, and future research should be directed to study and investigate the functional characteristics of Sample 3 (0/45/0-degree KF/SF/GF) laminates with more than 3 wt% SiO_2.

4 Conclusion

The epoxy composite laminates were prepared by different stacking of kenaf fiber (KF)/sisal fiber (SF)/glass fiber (GF) without and with 3 wt% silicon dioxide (SiO_2) nanoparticles via hot compression mold production method, and their microstructure, mechanical, moisture absorption, and thermogravimetric analysis were investigated. All important findings are summarized below.

- The fiber stacking position, interface structure, and the presence of the nano-SiO_2 nanoparticles in the epoxy hybrid composite laminates were confirmed via scanning electron microscope analysis.
- Among the various composites, Sample 3 (0/45/0-degree KF/SF/GF) laminates with 3 wt% SiO_2 showed higher mechanical, moisture, and thermal stability.
- The tensile, flexural, impact strength, and moisture absorption resistance of Sample 3 (0/45/0-degree KF/SF/GF) laminates with 3 wt% SiO_2 is 28%, 32%, 34.7%, and 45.8% higher than the epoxy composite (0/45/0-degree KF/SF/GF) laminates without nano-SiO_2 nanoparticles.
- Similarly, the thermal stability of sample 3 (0/45/0-degree KF/SF/GF) laminates with 3 wt% SiO_2 is 4.4% improved T_{onset} compared to the epoxy composite (0/45/0-degree KF/SF/GF) laminates without nano-SiO_2 nanoparticles.

Author Contributions All the authors contributed to the study's conception and design. Material preparation, data collection, and analysis were carried out by C. Gnanavel, Sathukumati Leela Lakshmi, Nirmith Kumar Mishra, Ayinala Naga Sai, Karvendhan S, S. Prabagaran, S. Jothi Arunachalam, Ramya Maranan, Anand Rajendran, and S Sathiyamurthy. The first manuscript draft was prepared by S. Jothi Arunachalam, and subsequently, all the authors contributed to the finalization of the manuscript.

Funding The authors did not receive support from any organization for the submitted work. No funding was received to assist with the preparation of this manuscript. No funding was received for conducting this study. No funds, grants, or other support were received.

Data Availability All the data required are available within the manuscript.

Declarations

Conflict of interests The authors have no relevant financial or non-financial interests to disclose. The authors have no competing interests to declare relevant to this article's content. All authors certify that they have no affiliations with or involvement in any organization or entity with any financial or non-financial interest in the subject matter or materials discussed in this manuscript. The authors have no financial or proprietary interests in any material discussed in this article.

Ethics Approval This is an observational study. Production and influence of SiO_2 and fiber sequencing on the mechanical and thermal properties of kenaf/sisal/glass laminates. The Research Ethics Committee has confirmed that no ethical approval is required.

References

1. S. Mahboubizadeh, A. Sadeq, Z. Arzaqi, O. Ashkani, M. Samadoghli, Advancements in fiber-reinforced polymer (FRP) composites: an extensive review. Discov. Mater. (2024). https://doi.org/10.1007/s43939-024-00091-9
2. R. Venkatesh, S. Raghuvaran, M. Vivekanandan, C.R. Kannan, T. Thirugnanasambandham, A. Murugan, Evaluation of thermal adsorption and mechanical behaviour of intralaminar jute/sisal/E-glass fiber-bonded epoxy hybrid composite as an insulator. Adsorpt. Sci. Technol.: Interface Sci. Adv. Mater. Technol. (2023). https://doi.org/10.1155/2023/9222562
3. A.B.M. Supian, M.R.M. Asyraf, A. Syamsir, Q. Ma, K.Z. Hazrati, M.N.M. Azlin, M. Mubarak Ali, A. Ghani, L.S. Hua, S. SaifulAzry, M.R. Razman, Z. Ramli, N.M. Nurazzi, M.N.F. Norrrahim, S.M.K. Thiagamani, Kenaf/glass fiber-reinforced polymer composites: pioneering sustainable materials with enhanced mechanical and tribological properties. Polym. Compos. **45**(16), 14421–14447 (2024). https://doi.org/10.1002/pc.28785
4. S.V. Prabhu, N. Nagabhooshanam, P.S. Parihar, N. Kedia, H.J. Christy, G. Satya, R. Maranan, T. Thirugnanasambandham, S. Sathiyamurthy, Fiber sequential action and combinations of nanographene and multi-walled carbon nanotubes on characteristics study of sustainable composite laminates. Iran. Polym. J. (2026). https://doi.org/10.1007/s13726-026-01698-w
5. V. Boobalan, T. Sathish, Evaluation of mechanical, morphological, and dynamic mechanical properties on basalt/E-glass fiber/epoxy modified with MWCNTs + SiO_2 hybrid nanocomposites. J. Polym. Res. (2024). https://doi.org/10.1007/s10965-024-04030-3
6. L. Jiang, Y. Yang, J. Sheng, Y. Li, Z. Huang, J. Li, T. Geng, Effects of different nano-SiO_2/silane coupling agent "rigid-flexible" hybrid interfaces on the mechanical performance of basalt fiber/epoxy composites. Polym. Compos. **46**(8), 6956–6969 (2025). https://doi.org/10.1002/pc.29406
7. M. Prashanth, S. Ramesh, P.S. Shivakumar Gouda, G.M. Naik, P. Sharma, C. Jagadeesh, M.M. Math, G. Anne, Impact of ply stacking sequence on the mechanical response of hybrid Jute-Banana fiber phenoplast composites. Materials Research Express **11**(5), 055301 (2024). https://doi.org/10.1088/2053-1591/ad425c
8. J.A. Solairaju, S. Rathinasamy, V. Rathinavelu, Silicon dioxide intermediate layer action on functional properties of jute/kenaf/glass fibers hybrid composites made with the compression route. Iran. Polym. J. **35**(3), 469–482 (2026). https://doi.org/10.1007/s13726-025-01532-9
9. S. Thanikodi, S.J. Arunachalam, R. Saravanan, J. Giri, M. Azizi, A.O. Hourani, F. Nasri, Characterization of mechanical, morphological, and dynamic mechanical properties of jute/Kenaf/glass fiber/epoxy modified with various nanofiller hybridized nanocomposites. Eng. Rep. (2025). https://doi.org/10.1002/eng2.70026
10. N.R. Prakash, C. Gnanavel, Investigation of quartz-rich granite dust particle-reinforced aluminized glass–kenaf fiber-reinforced polyester composite: load bearing, water absorption and flame properties. Fibers Polym. (2024). https://doi.org/10.1007/s12221-024-00671-9
11. G. Ananth, S. Thirugnanam, S. Rajaram, Load-bearing and machining behaviour of treated nano-sorghum-millet-husk-biosilica- and kenaf-fiber-reinforced vinyl ester composite. Fibers Polym. **25**(11), 4387–4399 (2024). https://doi.org/10.1007/s12221-024-00736-9
12. M.D. Albaqami, Y.D. Dwivedi, N. Krishnamoorthy, M.L. Kumar, L.H. Manjunatha, C.M. Chowdary, S.M. Wabaidur, A.R. Prasad, R.V. Chikhale, S.P. Kumar, Investigation on mechanical and thermal properties of a kenaf/jute fiber-reinforced polyester hybrid biocomposite. Adv. Polym. Technol. (2022). https://doi.org/10.1155/2022/7408135
13. R. Verma, M. Shukla, D.K. Shukla, Effect of glass fiber hybridization on the mechanical properties of unidirectional, alkali-treated kenaf-epoxy composites. Polym. Compos. **43**(10), 7483–7499 (2022). https://doi.org/10.1002/pc.26835
14. M.N.M. Azlin, S.M. Sapuan, M.Y.M. Zuhri, E.S. Zainudin, R.A. Ilyas, Thermal stability, dynamic mechanical analysis and flammability properties of woven kenaf/polyester-reinforced polylactic acid hybrid laminated composites. Polymers **14**(13), 2690 (2022). https://doi.org/10.3390/polym14132690
15. S. Shetty, S.S. Salins, H.K. Sachidananda, Design and characterization of natural fiber reinforced cotton-epoxy composites. Discov. Appl. Sci. (2024). https://doi.org/10.1007/s42452-024-06402-2
16. R. Venkatesh, Development and behavior analysis of CNT fibers reinforced high-density polyethylene composite via compression mold route. J. Inst. Eng. (India) Series D (2024). https://doi.org/10.1007/s40033-024-00718-4
17. A.S. Alvarez Lozano, A.I. Martínez Pérez, E.E. Vera Cárdenas, J.M. González Carmona, A. Mendoza Galván, Erosive wear behavior of fiberglass-reinforced epoxy laminate composites modified with SiO_2 nanoparticles fabricated by resin infusion. Lubricants (Basel, Switzerland) **14**(2), 65 (2026). https://doi.org/10.3390/lubricants14020065
18. S.A. Rafiqah, N. Abdullah, K. Abdan, M.H.M. Roslim, M.N. Radzuan, Influence of alkali treatment on mechanical, physical, thermal and morphological properties of Kenaf fiber/polyamide 6 composites. J. Nat. Fibers (2025). https://doi.org/10.1080/15440478.2025.2515468
19. D.P. Sahu, S.C. Mohanty, Static and dynamic analysis of polyethylene terephthalate foam core and different natural fiber-reinforced laminated composite-based sandwich plates through experimental and numerical simulation. Mech. Adv. Mater. Struct. (2024). https://doi.org/10.1080/15376494.2024.2388275
20. D.R. Rajkumar, A.R. Saravanan, N. Rachchh, R. Rajendran, S. Vijayakumar, N. Patil, A. Kashyap, A. Karthikeyan, H.P. Pydi, Mechanical and environmental performance of laminated composite plates reinforced with natural and synthetic fibers: a comparative study of flexural, water absorption and swelling characteristics. Discover Sustain. (2025). https://doi.org/10.1007/s43621-025-01550-w
21. B. Devarajan, R. Lakshminarasimhan, A. Murugan, S.M. Rangappa, S. Siengchin, D. Marinkovic, Recent developments in natural fiber hybrid composites for ballistic applications: a comprehensive review of mechanisms and failure criteria. Facta Univ. Ser. Mech. Eng. (2024). https://doi.org/10.22190/fume240216037d
22. M. Alhijazi, Q. Zeeshan, B. Safaei, M. Asmael, Z. Qin, Recent developments in palm fibers composites: a review. J. Polym. Environ. **28**(12), 3029–3054 (2020). https://doi.org/10.1007/s10924-020-01842-4
23. A. Abdelhussien, G. Yang, E.K. Hussein, L. Li, H. Al-Abboodi, B. Mohamad, Analysis of the mechanical characteristics of date seed powder-based composite carbon fiber reinforced polymers. Facta Univ. Ser. Mech. Eng. **23**(2), 251 (2025). https://doi.org/10.22190/fume230728040a
24. M. Alhijazi, B. Safaei, Q. Zeeshan, M. Asmael, M. Harb, Z. Qin, An experimental and metamodeling approach to tensile properties of natural fiber composites. J. Polym. Environ. **30**(10), 4377–4393 (2022). https://doi.org/10.1007/s10924-022-02514-1
25. M. Alhijazi, B. Safaei, Q. Zeeshan, S. Arman, M. Asmael, Prediction of elastic properties of thermoplastic composites with natural fibers. J. Text. Inst. (2022). https://doi.org/10.1080/00405000.2022.2131352
26. M. Alhijazi, B. Safaei, Q. Zeeshan, M. Asmael, Modeling and simulation of the elastic properties of natural fiber-reinforced thermosets. Polym. Compos. **42**(7), 3508–3517 (2021). https://doi.org/10.1002/pc.26075

27. S. Esmaeili, H. Akbari Aghdam, M. Motififard, S. Saber-Samandari, A.H. Montazeran, M. Bigonah, E. Sheikhbahaei, A. Khandan, A porous polymeric-hydroxyapatite scaffold used for femur fractures treatment: fabrication, analysis, and simulation. Eur. J. Orthop. Surg. Traumatol. **30**(1), 123–131 (2020). https://doi.org/10.1007/s00590-019-02530-3
28. S. Foroutan, M. Hashemian, M. Khosravi, M.G. Nejad, A. Asefnejad, S. Saber-Samandari, A. Khandan, A porous sodium alginate-CaSiO3 polymer reinforced with graphene nanosheet: fabrication and optimality analysis. Fibers Polym. **22**(2), 540–549 (2021). https://doi.org/10.1007/s12221-021-0347-9
29. M. Aruna, N. Nagabhooshanam, R. Kumar, J. Jagtap, S. Sunitha, B.E.V.L. Naidu, R. Siriyala, M. Murali, S. Sathiyamurthy, Integration of carbon nanotube and epoxy coupling agent on microstructural and functional characteristics of polyimide composites. Iran. Polym. J. **35**(7), 1515–1524 (2026). https://doi.org/10.1007/s13726-026-01604-4
30. T. Premkumar, N. Nagabhooshanam, P.S. Parihar, N. Bhosle, S. Supriya, V.S.N. Kumar, D. Barik, R. Srinivasan, S. Sathiyamurthy, Enrichment of poly-fiber composites functional properties by the influences of hydrophobic titanium dioxide nanoparticles via injection mould technique. Iran. Polym. J. **35**(6), 1245–1259 (2026). https://doi.org/10.1007/s13726-025-01586-9

Authors and Affiliations

C. Gnanavel[1] · Sathukumati Leela Lakshmi[2] · Nirmith Kumar Mishra[3] · Ayinala Naga Sai[4] · S. Karvendhan[5] · S. Prabagaran[6] · S. Jothi Arunachalam[7] · Ramya Maranan[8] · Anand Rajendran[9] · S. Sathiyamurthy[10]

✉ S. Jothi Arunachalam
jothiaruna.19@gmail.com

C. Gnanavel
gnanavelmech1986@gmail.com

Sathukumati Leela Lakshmi
satleelavit06@gmail.com

Nirmith Kumar Mishra
nirmithmishra@gmail.com

Ayinala Naga Sai
ayinala.nagasai.civil113@gmail.com

S. Karvendhan
karvendhans@gmail.com

S. Prabagaran
s.prabagaran.cbe@gmail.com

Ramya Maranan
ramyamaranan451@gmail.com

Anand Rajendran
dranandrajendran@yahoo.com

S. Sathiyamurthy
ssathya1978@gmail.com

[1] Department of Mechanical Engineering, Vels Institute of Science, Technology and Advanced Studies, Pallavaram, Chennai, Tamil Nadu 600117, India

[2] Department of Electronics and Communications Engineering, Vemu Institute of Technology, P.Kothakota, Chittoor District, Andhra Pradesh 517112, India

[3] Department of Aeronautical Engineering, MLR Institute of Technology, Hyderabad, Telangana, India

[4] Department of Civil Engineering, Aditya University, Surampalem, Andhra Pradesh 533437, India

[5] Department of Mechanical Engineering, Velalar College of Engineering and Technology, Erode, Tamil Nadu 638012, India

[6] Department of Mechanical Engineering, Karpagam Academy of Higher Education, Coimbatore, Tamil Nadu 641021, India

[7] Department of Mechanical Engineering, Saveetha School of Engineering, Saveetha Institute of Medical and Technical Sciences, SIMATS, Chennai 602105, Tamil Nadu, India

[8] Division of Research and Development, Lovely Professional University, Jalandhar, Delhi, G.T. Road, Phagwara, Punjab 144411, India

[9] Lloyd Institute of Engineering and Technology, Plot No. 3, Knowledge Park II, , Greater Noida, Uttar Pradesh 201306, India

[10] Jerusalem College of Engineering, Pallikaranai, Chennai, Tamil Nadu 600100, India